

# Flow disturbance characterization of highly filled thermoset injection molding compounds behind an obstacle and in a spiral flow part

Ngoc Tu Tran <sup>1\*</sup>, Andreas Seefried <sup>1</sup>, Michael Gehde <sup>1</sup>, Jan Hirz <sup>2</sup> and Dietmar Klaas <sup>2</sup>

<sup>1</sup> Professorship of Plastics Technology, Department of Mechanical Engineering, Chemnitz University of Technology, 09126 Chemnitz, Germany; kunststoffe@mb.tu-chemnitz.de

<sup>2</sup> Baumgarten automotive technics GmbH, Carl-Benz Straße 46, 57299 Burbach, Germany; info@bat-duro.com

\* Correspondence: ngoc-tu.tran@mb.tu-chemnitz.de or ngocagvt@gmail.com

**Abstract:** In the injection molding process weld-line regions occur when a molten polymer flow front is firstly separated and then rejoined. The position, the length and the angle of weld-lines are dependent on the gate location, the injection speed, the injection pressure, the mold temperature and especially the direction and degree of the polymer melt velocity in the mold filling process. However, the wall surface velocity of thermoset melt in the mold filling process is different from zero, which is not found for the thermoplastic injection molding. The main reason leads to this difference is the slip phenomenon in the filling phase between the thermoset melt and wall surface, which is directly affected by filler content. In this study, commercial thermoset phenolic injection molding compounds with different amount of filler were employed to investigate not only the mechanism of weld-lines formation and development behind an obstacle in the injection molding process, but also the flow disturbance of thermoset melt in a spiral flow part. In addition, the effect of the wall slip phenomenon on the flow disturbance characterization and the mechanism of weld-lines of selected thermoset materials is carefully considered in this research. Furthermore, the generated material data sheet with the optimal developed reactive viscosity and curing kinetics model was imported into a commercial injection molding tool to predict the weld-lines formation as well as the molding filling behavior of selected thermoset injection molding compounds such as the flow length, the injection pressure gradient, the temperature distribution and the viscosity variation. The results obtained in this paper provide important academic knowledge about the flow disturbance behavior and as well as its influence on the mechanism of the weld-lines formation in the process of thermoset injection molding. Furthermore, the simulated results were compared to the experimental results, which helps us to have an overview about the ability of the computer simulation in the field of reactive injection molding process.

**Citation:** To be added by editorial staff during production.

Academic Editor: Firstname Last-name

Received: date

Revised: date

Accepted: date

Published: date



**Copyright:** © 2023 by the authors. Submitted for possible open access publication under the terms and conditions of the Creative Commons Attribution (CC BY) license (<https://creativecommons.org/licenses/by/4.0/>).

**Keywords:** Thermoset molding compounds; Injection molding; Plug flow; Fountain flow; Filler content; Weld-line; Computer simulation; Surface roughness; Wall slip; Pressure sensor; Infrared temperature sensor.

## 1. Introduction

Thermoset materials are used in various applications in which high thermo-mechanical, chemical and electrical properties are required [1, 2]. These applications include, specifically, automotive, aerospace, and electronics [3, 4]. Thermoset polymer parts could be processed by various methods which are compression molding, transfer molding, injection compression molding or injection molding. However, the injection molding method that is defined by a cycle and automated process for manufacturing identical plastic articles from mold, is the most widely used [5]. Small or very large parts could be manufactured by the injection molding method. In this process, the thermoset molding

compounds are plasticized at temperatures between 90 and 100 °C and then injected into a hot mold with the temperature at 160 to 190 °C [6].

Weld-line is one of popular problems that always appears in the injection molding process. It is the line formed by two or more different melt fronts joining together with sharp angle during the mold filling stage. It decreases the strength of the final molded products and produce cosmetic defect [7]. Most of the previously stated publications related to the weld-line formation and weld-line strength in injection molded parts are conducted on thermoplastics materials [8-11]. For example, there are three main factors which influences strongly the weld-line strength of thermoplastics [12], including high orientation of the macromolecules and fillers parallel to the weld-line, lack of diffusion of the macromolecules between two melt front surfaces and stress concentrations because of notches on the surface next to the weld-line. The influence of processing parameters on the thermoplastic weld-line strength was investigated [13, 14]. It was found that the melt and mold temperature have great influence on these properties. In addition, the reduction of weld-line strength of unreinforced, amorphous thermoplastics was investigated, analyzed and calculated by a physical model of molecular diffusion [15]. The experimental results shown that a combination of low holding pressure and high melt temperature should be selected to improve weld-line strength. Furthermore, the notch structure of polystyrene was studied by Tomari [16] and it was reported that different bonding strengths are dependent on the depth of notches.

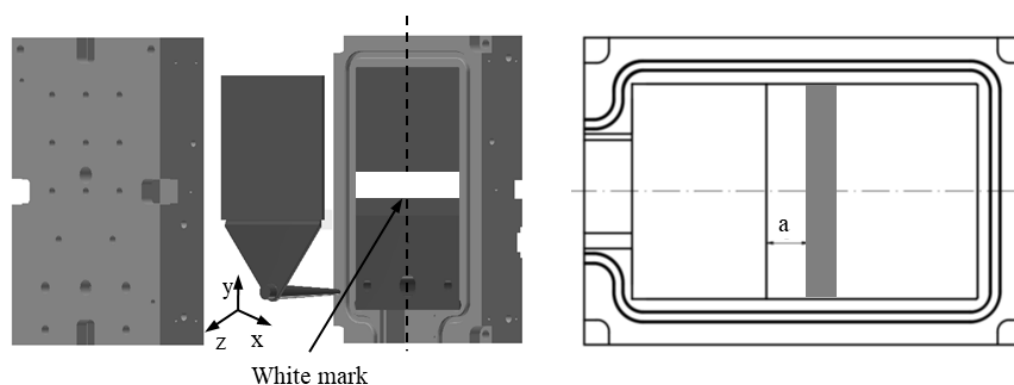


Figure 1. A simple standard two-plate mold with the location of painted white marks [23]

However, the previously stated knowledge on mechanism of weld-line formation of thermoplastics materials could be only partially applicable for highly filled thermoset injection molding compounds [17]. Because the previously articles published by authors show that the mold filling behavior of highly filled thermoset injection molding compounds is completely different from thermoplastic materials. Specifically, the mold filling characterization of these materials in the injection molding process is a plug flow [18-23] instead of fountain flow which is found for thermoplastic materials. In the filling phase of the injection molding process, there is a strong slip phenomenon between the thermoset melt and wall surface, which is not found for the injection molding of thermoplastic materials. In addition, the effect of filler content, the processing condition, such as the mold temperature, the injection speed and the surface roughness on the polymer filling behavior in the thermoset injection molding process [23] was successfully investigated and analyzed by using the mold printing method, as shown in [Figure 1]. The slip phenomenon between thermoset melt and the mold wall surface was studied and explained via analysis of the visualizable movement of the thermoset melt dyed white color on the surface of the injection molded parts. All received experimental results shown that the filler amount, the injection speed, the mold temperature, and the surface roughness have great influence on the wall slip phenomenon of phenolic thermoset injection molding compounds in the filling phase. A lower filler amount and injection speed; a higher mold temperature and

surface roughness decrease the wall slip phenomenon of the thermoset melts. Because of this wall slip phenomenon, the velocity profile of molten thermoset on the interface between thermoset melt and mold wall surface must be different from zero [23] that is completely different from the velocity profile of molten thermoplastic materials. Consequently, the mechanism of weld-line formation and development of high-filled thermoset melt in the filling phase is different from the previously stated knowledge on the theory about the weld-line formation of thermoplastic materials. However, this problem has not yet been carefully investigated and published in any scientific article.

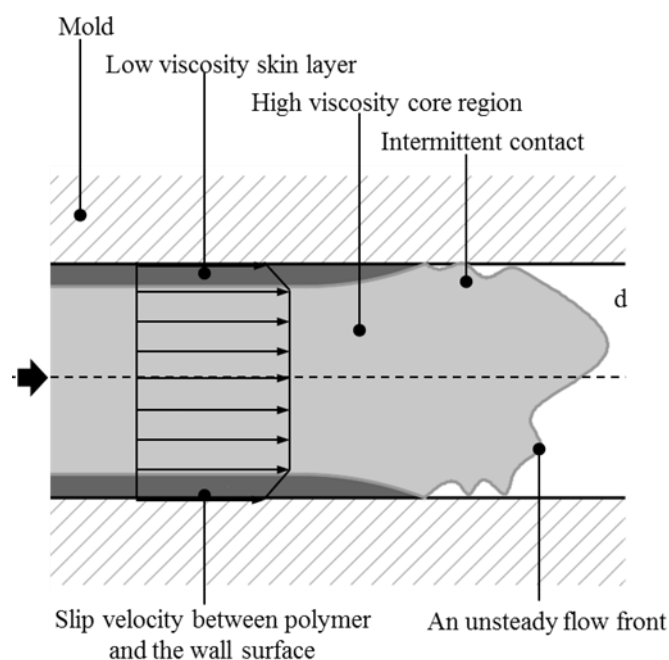


Figure 2. Velocity behavior of high-filled thermoset injection molding compounds in the mold filling process [23]

Nowadays, simulation software such as Moldex3D, Moldflow and SigmaSoft is widely being employed to simulate the all phases of the injection molding process [19, 20]. Potential problems in the filling phase of the injection molding process such as weld-line positions, air traps and sink marks which usually appear on the molded parts could be predicted. As a result, mistakes in designing process can be modified and the processing conditions such as injection speed, mold temperature, injection pressure and holding pressure could be optimized, which helps us to save the time as well as manufacturing cost. In order to simulate all phases of the injection molding process, it is necessary to define material data sheet that include the heat capacity and thermal conductivity, the viscosity data that consists of a viscosity model and fitted coefficients, a pressure-volume-temperature (PVT) data that must include a PVT model and fitted parameters. Especially, for the reactive injection molding simulation a curing kinetics model with fitted parameters are required [19-22].

$$\frac{\partial \rho}{\partial t} + \nabla \cdot \rho \mathbf{v} = 0 \tag{1}$$

$$\rho \frac{\partial \mathbf{v}}{\partial t} = \rho \mathbf{g} - \nabla p + \nabla \cdot \eta \mathbf{D} - \rho \mathbf{v} \cdot \nabla \mathbf{v} \tag{2}$$

$$c_p \left( \frac{\partial T}{\partial t} + \mathbf{v} \cdot \nabla T \right) = \beta T \left( \frac{\partial p}{\partial t} + \mathbf{v} \cdot \nabla p \right) + \eta \dot{\gamma}^2 + k \cdot \nabla^2 T \tag{3}$$

The fluid dynamic equations, including the conservation of mass, momentum and energy, as shown respectively from Equations (1-3) are employed to write the simulation code for characterizing the molding filling behavior of polymer melt in the injection molding process [19, 20]. In these equations  $\eta$  is viscosity,  $\rho$  is density,  $c_p$  is heat capacity,  $k$  is thermal conductivity,  $T$  is temperature,  $v$  is velocity vector,  $g$  is the total body force per unit mass, and  $\beta$  is coefficient of volume expansion. It could be seen from these equations that there are symbols which represent the material data sheet for the simulation process. Therefore, there will have a huge impact on the accuracy of predicted results [24] if there is any change in the material data sheet. To improve the simulated results, it requires a fitting tool that is used to import the measured material data for the injection molding simulation software.

The material data sheet for the thermoplastic injection molding simulation process is always available from material manufacturers or already added in the material data bank of the commercial injection molding simulation software [5, 19, 20]. In contrast, the material data sheet of almost currently commercial highly filled thermoset injection molding compounds is unavailable from material suppliers and seldomly embedded in the material data bank of the commercial simulation software. Because the rheological and thermal properties such as viscosity, curing kinetics behavior are difficult to measure [19, 20]. For example, viscosity of thermoset materials is not only dependent on the temperature and shear rate like thermoplastics materials, but also dependent on the curing behavior. In addition, if the material data of thermoset materials could be successfully measured, modelling of rheological and thermal data for the reactive injection molding simulation process will require extensive knowledge not only in creating reactive viscosity models, but also in the field of optimization algorithm. These existing problems are being solved step by step by authors [19-22].

With profound knowledge in the field of rheological and thermal properties [20, 25, 26], viscosity, curing kinetics, thermal conductivity and heat capacity of thermoset injection molding compounds have been successfully studied and measured by authors [19-21]. In addition, based on the measured rheological and thermal data, the numerical method was developed to generate the material data sheet for the thermoset simulation process. This innovation won the special prize at the Moldex3D Global Innovation Talent Award 2018. These fitted processing coefficients were integrated into a cure kinetics model, the Kamal model, and a reactive viscosity model, the Cross-Castro-Macosko model, which were used to simulate the reactive injection molding process [19, 20].

Although, a complete way to create thermoset material data from measured experimental data (thermal data and rheological data) for the reactive injection molding simulation process was successful studied by authors [20], there are things which should be further studied. In the process of creating material data the developed numerical method is based only on a cure kinetic model, namely Kamal model, and a reactive viscosity model, namely Cross-Castro-Macosko model while there are still other cure kinetics and reactive viscosity models. In contrast, a comparison of the efficiency to use each cure kinetics model and reactive viscosity model to describe cure kinetics data and rheological data respectively has not yet been done. If this could be done, a thermoset material data sheet for the reactive simulation process could be created with the best cure kinetics and reactive viscosity model. In order to solve this problem, a complete fitting tool, namely Thermoset - TU - Fitting Tool [21, 22], was successfully developed and written. In the writing process the least-square estimation algorithm developed by Levender- Marquardt (LMA) [27] and embedded in Matlab program language was used. The Thermoset - TU - Fitting Tool was employed as a useful tool for transporting the experimental rheological and thermal data to the any injection molding simulation software. With the Thermoset - TU - Fitting tool, an evaluation of developed reactive viscosity and cure kinetics models that are currently used for rheological and thermal simulation in the thermoset injection molding process was successfully carried out. The reactive viscosity models include Castro Macosko Model, Cross-Castro-Macosko Model, Power-Law\_Castro\_Macosko Model

and Herschel-Bulkley-WLF- Castro- Macosko model [21, 22]. The cure kinetic models consist of Kamal model, Modified Kamal model, Deng Isayev model and Grindling model [21, 22].

By dint of using the developed Thermoset - TU - Fitting tool [21, 22] it was found that all presented reactive viscosity and cure kinetics models could be used to describe the reactive viscosity and cure kinetics data well. In the case of curing kinetics models, the best curing model is still the previously used Kamal model. However the reactive viscosity model, Herschel-Bulkley-WLF- Castro- Macosko Model (Herschel-Bulkley model), describes and fits the the parabolic curve of the experimental viscosity property the best instead of the previously used Cross-Castro-Macosko model. Because the viscosity of selected thermoset materials at the low temperature is successfully simulated by the Herschel-Bulkley-WLF- Castro- Macosko Model, which is not the case in other reactive viscosity models. The main reason that leads to the difference in adaptation of reactive viscosity models in characterization of viscosity is the yield stress phenomenon of high filled plastics [22]. In the Herschel-Bulkley-WLF- Castro- Macosko Model there is a coefficient ( $\tau_y = \tau_{y0} \cdot \exp\left(\frac{T_y}{T}\right)$ ) that shows the influence of yield stress phenomenon on the viscosity of high filled thermoset injection molding compounds. Therefore, the generated Herschel-Bulkley-WLF- Castro- Macosko Model describes and fits the experimental reactive viscosity data of high filled thermoset materials the best. Consequently, the optimal reactive viscosity model and cure kinetics model were found and employed to generate the material data sheet of commercial high-filled thermoset materials for the reactive simulation process [21, 22].

Based on the gained results and the existing problems, the present article focuses on two scientific key goals. On the one hand, the aim is to continuously understand and explain the physical filling behavior of reinforced thermoset injection molding compounds such as flow length, the influence of the wall slip and flow disturbance behavior on the mechanism of weld-line formation, the pressure gradient, the temperature distribution, the viscosity characterization and the degree of cure. On the other hand, the generated material data sheet with the optimal reactive viscosity and cure kinetics model will be employed to investigate the application of the commercial injection molding simulation software in simulation of mold filling behavior of highly filled thermoset injection molding compounds.

## 2. Materials and methods

### 2.1. Injection molding process

#### 2.1.1. Highly filled thermoset injection molding compounds

Bakelite PF6680, Bakelite PF6506, Bakelite PF1110 are three commercial thermoset phenolic injection molding compounds with different filler content for the injection molding process, which were selected and ordered from a material supplier. The filler content is from 55% to 80%, as shown in Table 1.

**Table 1.** Experimental materials.

Abbreviation	Commercial Name	Manufacturer
PF-GF25+GB30	Bakelite PF6680	Bakelite
PF-GF30+GB30	Bakelite PF6506	Bakelite
PF-GF35+GB45	Bakelite PF1110	Bakelite

#### 2.1.2. Studying objects

The study objects are three different parts. The first part is plate part with a hole (Figure 3). The dimension of plate part is 150 mm × 150 mm × 4 mm. The diameter of the hole as an obstacle is 8 mm. The plate part with the obstacle of 8 mm was used to investigate the influence of the filler content, the wall slip phenomenon and the processing conditions on the mechanism of weld-line formation and development in the mold filling

process. The second part is spiral flow part (Figure 4) which was used to investigate the flow disturbance characterization such the flow length, pressure gradient, temperature and viscosity behavior. The last part is complex part from industry, which was employed to study both flow disturbance characterization and weld-line positions.

### 2.1.2. Experimental procedure

A hydraulic Krauss Maffei injection molding machine KM 150-460B, with a screw diameter of 45 mm and a three-zone plasticizing cylinder, was employed to do injection molding process of the plate part with the obstacle and the spiral flow part.

Firstly, a simple standard two-plate mold was employed to study the weld-lines formation mechanism of selected materials. In the experimental process, the mold painting method developed by authors and published in the previous articles continues to be employed [23]. The white mark was painted on the constant position of the mold wall surface. The schematic position of the constant rectangular white mark which was painted on the wall surface of the mold is shown in Figure 1. The distance (a) of 20 mm between the location of the white mark and the boundary line between the cavity and the film gate is constantly kept in all experimental processes. The injection molding experiments of three chosen phenolic injection molding compounds were conducted. The temperature profile in the injection chamber (cylinder temperature) is 100 °C-80 °C-60 °C. The mold temperature of 175 °C is constantly kept under different injection speeds of 8 cm<sup>3</sup>/s, 16 cm<sup>3</sup>/s, and 32 cm<sup>3</sup>/s. In order to get more information for analyzing the mechanism of weld-lines formation and development behind the obstacle, a series of incomplete molded parts with different percentages of cavity volume was conducted.

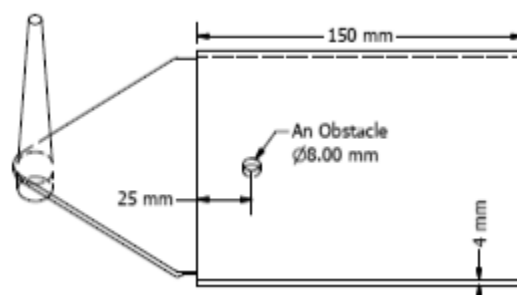


Figure 3. The plate part with a film gate and an obstacle

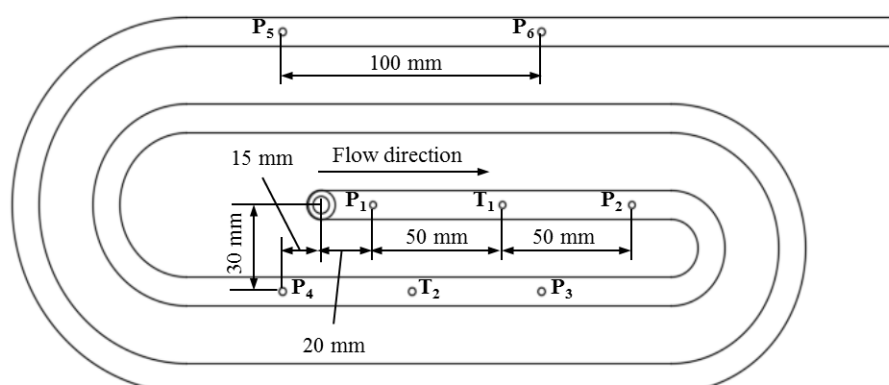


Figure 4. The spiral part; the location of six pressure sensors from P<sub>1</sub> to P<sub>6</sub> and two infrared temperature sensors T<sub>1</sub> and T<sub>2</sub>

Secondly, to analyze flow disturbance behavior and the wall slip phenomenon of highly filled thermoset injection molding compounds further, the spiral flow with the flow length of 1385 mm was used for the next experiments. With the spiral flow part, it is

possible to study the influence of the chemical reaction on the viscosity, which effects the flow length. In addition, the variation of the polymer temperature and pressure during the filling phase will be analyzed by using pressure and infrared temperature sensors that are set on the interface between thermoset melt and wall surface. Based on the temperature gradient, the generation of heat by chemical reactions and the heat transfer from the mold to the polymer melt will be analyzed. In this step, only two phenolic injection molding compounds with the lowest and highest filler content which are Bakelite PF6680 (55% filler) and Bakelite PF1110 (80% filler) were selected to conduct spiral injection molding experiments. The temperature profile in the injection chamber (cylinder temperature) is 100 °C-80 °C-60 °C. There injection speed profile in the screw is 6-10-12 cm<sup>3</sup>/s, which is constantly kept. The mold temperature is 160 °C, 175 °C and 190°C respectively.

Finally, the complex industrial part from Baumgarten automotive technics GmbH, Carl-Benz Straße 46, 57299 Burbach, Germany was employed to study the flow length as well as the location of weld-lines. Because of commercial reason, all information about name of material, geometry of the complex industrial part and the processing conditions is not presented in this article. In order to get more information about manufacturing process of the complex industrial part, please do not hesitate to contact Baumgarten automotive technics GmbH by email: [info@bat-duro.com](mailto:info@bat-duro.com)

## 2.2. Simulation process

### 2.2.1. Generating material data sheet for the injection molding simulation process

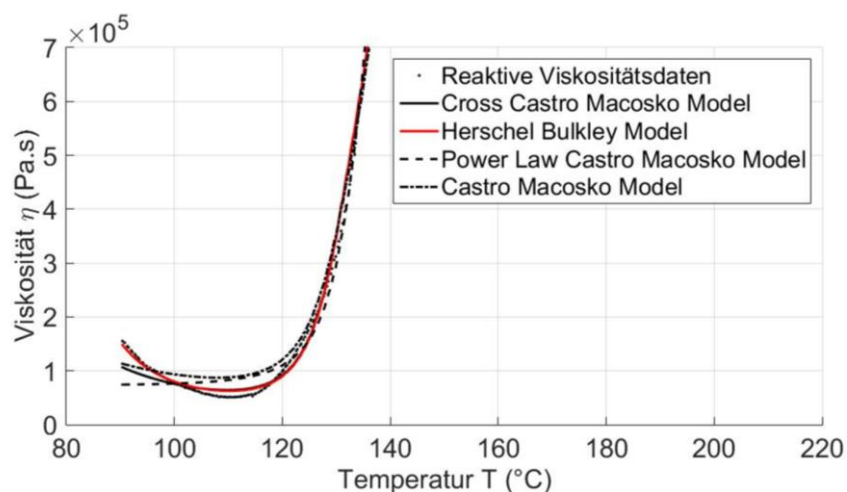


Figure 5. Modelling of reactive viscosity models for the injection molding simulation process

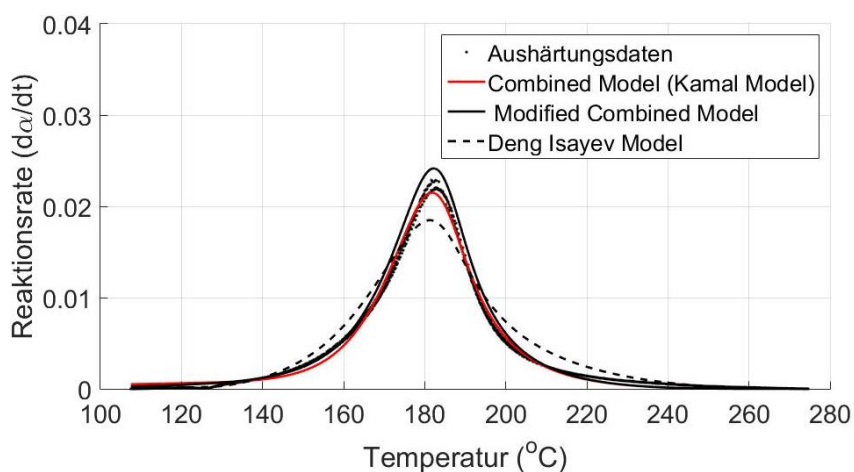


Figure 6. Modelling of cure kinetics models for the injection molding simulation process

The material data sheet of Bakelite PF6680, Bakelite PF6506, Bakelite PF1110 for the simulation process are now not available from the material manufacturers and not found in data bank of any commercial injection molding simulation software. Therefore, The Thermoset - TU - Fitting Tool that developed by authors [21, 22] was employed to generate the material data sheet of these selected materials. In the generated material data sheet for the simulation process, the optimal reactive viscosity model, Herschel-Bulkley-WLF- Castro- Macosko Model with fitted coefficients and the optimal cure kinetics model, Kamal model with fitted coefficients were employed to characterize the rheological and thermal properties, as shown in Figure 5 and Figure 6. To find out more information in the field of creating material data sheets for thermoset injection molding compounds, please refer to the international articles that were previously published by authors [19-22].

The task in this working package is therefore to export the generated material data sheet of these selected materials as input file for the next step, simulation process. An input file is generated for each material, which contains the value of heat capacity and the value thermal conductivity at different temperature; cure kinetics data that include Kamal model with fitted coefficients and reactive viscosity model that is Herschel-Bulkley-WLF- Castro- Macosko Model with fitted coefficients. All input files were imported in the commercial simulation software (Moldex3D) to predict the mold filling behavior of the selected thermoset materials.

#### 2.2.2. Simulation of the mold filling behavior

Moldex3D simulation will be selected to simulate the reactive injection molding process by the reason it implemented a high-performance finite volume method (HPFVM). This numerical method synergizes robustness and efficiency in contrast to the finite element method [20, 28]. The HPFVM of Moldex3D is called Designer Boundary Layer Mesh (BLM). This technique solves the transient flow field in three dimensions. It generates multiple layers of prismatic meshes inward from the surface mesh and then it is filling up the remaining space with a tetrahedral mesh. BLM can capture precisely the drastic changes of temperature and velocity near the cavity wall during the filling process. Also, it can help detecting viscous heating and warpage problems in advance accurately. In addition, with Moldex3D, the wall slip boundary condition is considered during the simulation process.

The simulation subjects are firstly the plate part (Figure 3) and then the spiral part (Figure 4), which were also used in the injection molding process. The processing conditions are the same with the experimental process. In addition, to show the practical benefit of both the generated material data sheet and injection simulation model, the simulation process is supposed to test the complex industrial part from Baumgarten automotive technics GmbH.

### 3. Results and Discussion

#### 3.1. Mechanism of weld-line formation and development behind an obstacle

Like in the previous publications [18, 20, 23], it could be seen from Figure 7 to Figure 9 that the thermoset melt dyed white color on the surface of the injected parts moves from the original painted position to near the melt front. The movement of the polymer dyed white color derives from the wall slip between the phenolic polymer and the mold wall surface. Nevertheless, the intensity of the white stripes is different on the surface of the molded parts, which is dependent on the percentage of reinforced filler. Specifically, the material, PF6680 with the lowest filler content (55 % filler), the white color still appears at the original painted position, as shown in Figure 7. However, for PF6506 with only more 5% filler, the density of white color (Figure 8) at the original painted position is lower and not clear as PF6680. In contrast, the material PF1110 with the highest filler content (80% filler), the white color does not appear at the original painted position (Figure 9). Based on the difference in thermoset melt dyed white color at the original painted position, it could be summarized that PF1110 (GF35+GB45) has the strongest slip phenomenon,



followed by PF6506 (GF30+GB30) and PF6680 (GF25+GB30). In addition, the amount of filler is the main factor that has a great impact in the wall slip phenomenon on the interface between the phenolic polymer and the mold wall surface. The wall slip phenomenon is stronger if the amount of filler increases.

Although the processing conditions are the same, the joining mechanism of melt fronts of the selected highly filled thermoset injection molding compounds behind the obstacle in the filling phase is completely different. Beginning with 40% Cavity volume, the melt fronts of PF6680 (Figure 7) and PF6506 (Figure 8) are immediately reunited behind the obstacle, which is not found in the mold filling behavior of PF1110 (Figure 9). When the Cavity volume increases only more 10%, the joined fronts of PF6680 (Figure 7, 50% Cavity) and PF6506 (Figure 8, 50% Cavity) slips in the flow direction. In contrast, the melt fronts of PF1110 are still not reunited and has a translation motion in the flow direction. As a result, there is still a gap without polymer between two melt fronts (Figure 9, 50% Cavity). The distance of the gap in the incomplete part molded from 50% Cavity is equal to or greater than the diameter of the obstacle (8 mm).

When increasing the injection volume that is 60%, 70%, 80% and 90 % respectively, the reunited melt fronts of PF6680 and PF6506 continues to move slightly in the flow direction. The position of weld-line is found in the middle line of complete molded part (100% Cavity), as shown in Figure 7 and Figure 8. However, this phenomenon is not found in the melt front behavior of PF1110. When the cavity volume is 60 % the melt fronts of PF1110 flow and slip not only in the flow direction but also in the perpendicular to the flow direction. Therefore, the distance of gap without polymer starts decreasing. Nevertheless, two melt fronts are still not reunited, which begins being joined as the cavity volume is higher (Figure 9 with 70% Cavity and 80% Cavity). The joining process of melt fronts is not complete because there are still different air gaps without polymer on the surface of molded parts, which means that there will be different small weld-line regions on the surface of complete plate molded part. Furthermore, the surface of this incomplete molded part is roughness and the molded parts is uncompacted. The melt fronts of PF1110 is completely joined with the cavity volumes of more than 90 %, which has an anisotropic motion.

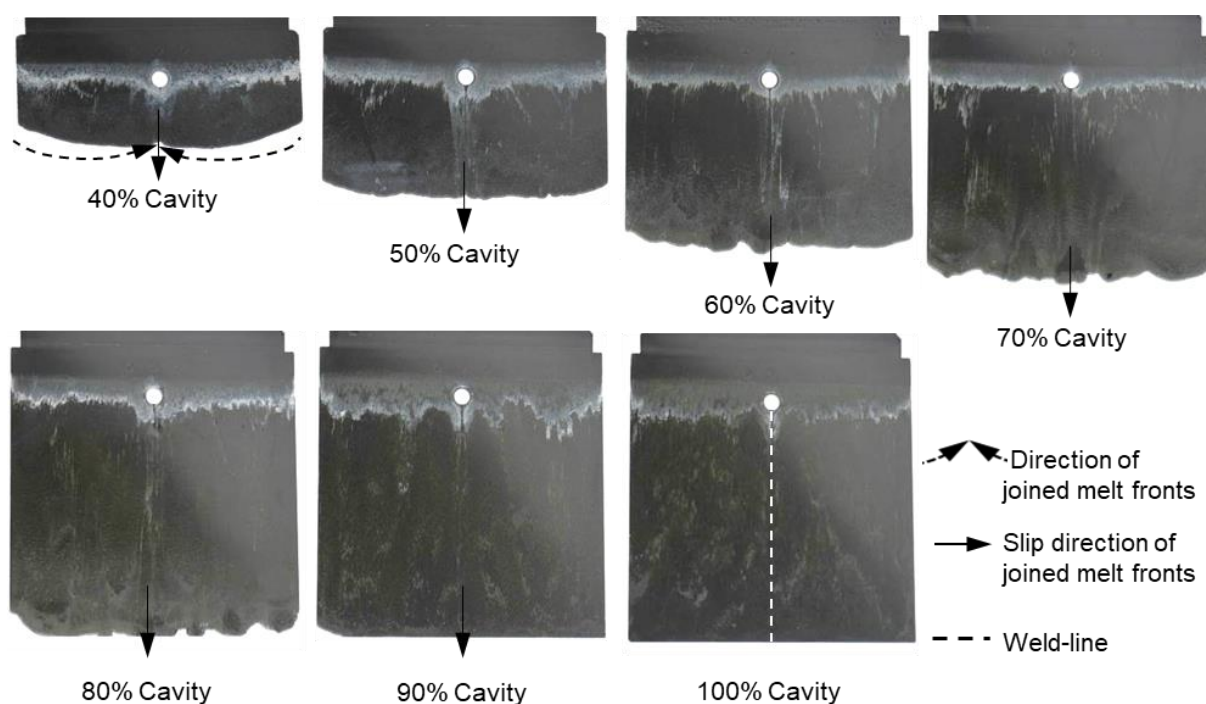


Figure 7. PF6680 (GF25+GB30); the mechanism for reuniting two melt fronts behind an obstacle. Mold temperature is 175 °C, and injection speed is 8 cm<sup>3</sup>/s.

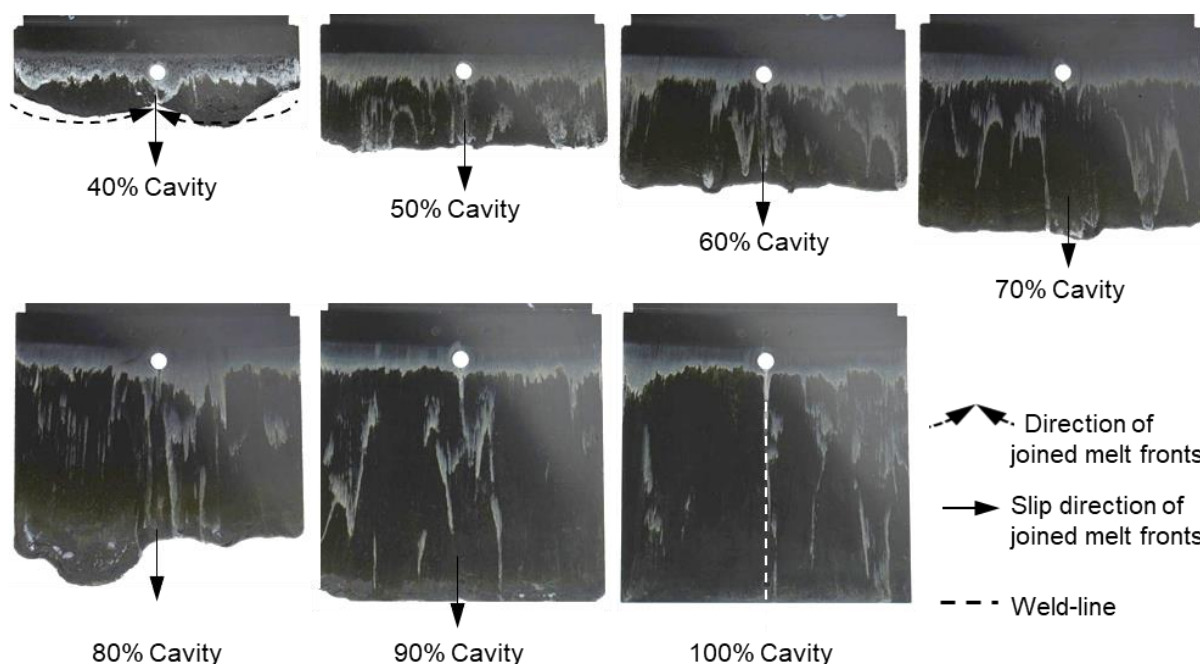


Figure 8. PF6506 (GF30+GB30); the mechanism for reuniting two melt fronts behind an obstacle. Mold temperature is 175 °C, and injection speed is 8 cm<sup>3</sup>/s.

348  
349  
350

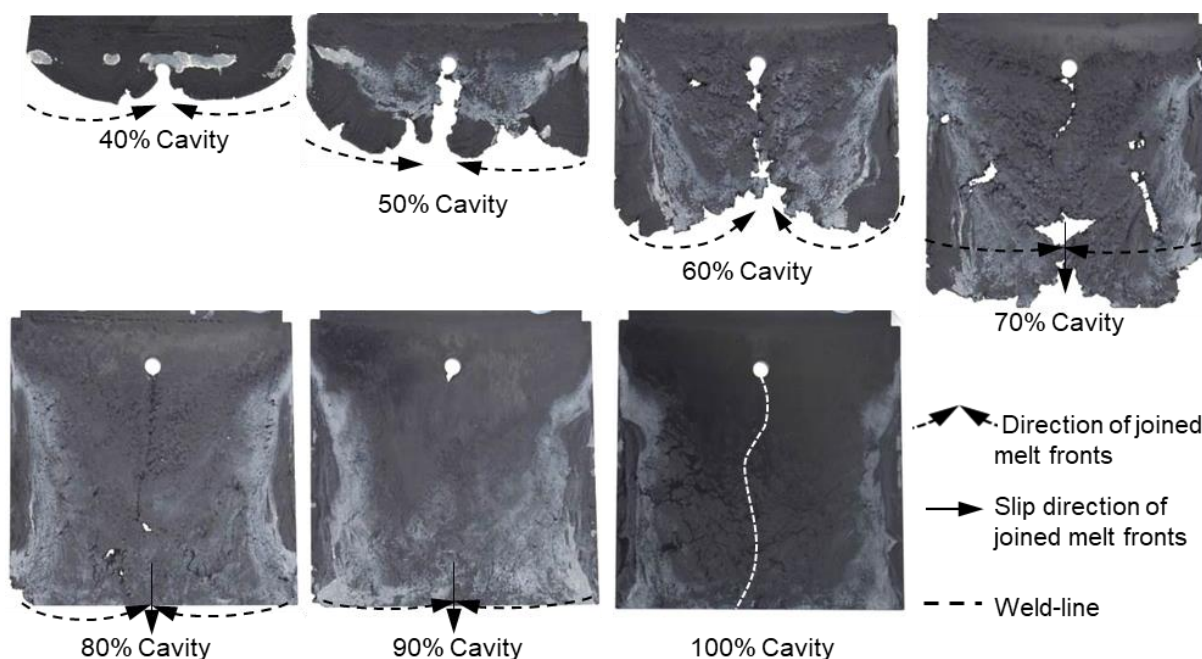


Figure 9. PF1110 (GF35+GB45); the mechanism for reuniting two melt fronts behind an obstacle. Mold temperature is 175 °C, and injection speed is 8 cm<sup>3</sup>/s.

351  
352  
353

### 3.2. Influence of injection speeds on the mechanism of weld-line formation and development

Figure 10 and Figure 11 show that although there is change in injection speed, the melt fronts of PF6680 und PF6506 is still immediately reunited behind the obstacle. The joined melt fronts slightly slip and move in the flow direction when the injection volume increases, as shown in Figure 12 and Figure 13. For all investigated injection speeds, the weld-line region is found in the middle line of plate molded part. Density of white color on the surface of molded parts shown that the slip degree of the joined melt fronts is stronger when increasing the injection speed.

354  
355  
356  
357  
358  
359  
360  
361

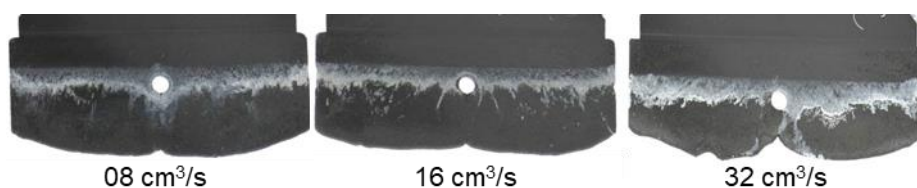


Figure 10. PF6680 (GF25+GB30); the influence of injection speeds on the joining mechanism of the melt fronts behind an obstacle. Mold temperature of 175 °C is constant and Cavity volume is 40%

362  
363  
364

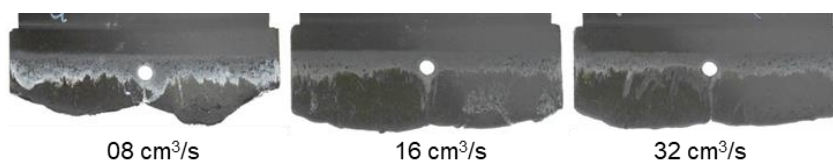


Figure 11. PF6506 (GF30+GB30); the influence of injection speeds on the joining mechanism of the melt fronts behind the obstacle. Mold temperature of 175 °C is constant and Cavity volume is 40%

365  
366  
367

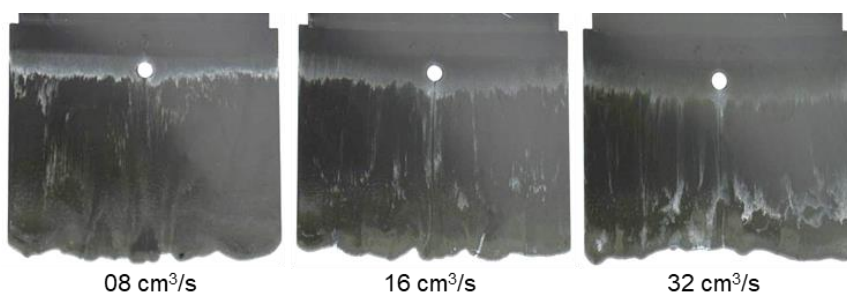


Figure 12. PF6680 (GF25+GB30); the mechanism for reuniting melt fronts behind the obstacle. Mold temperature of 175 °C is constant and Cavity volume is 70%

368  
369  
370

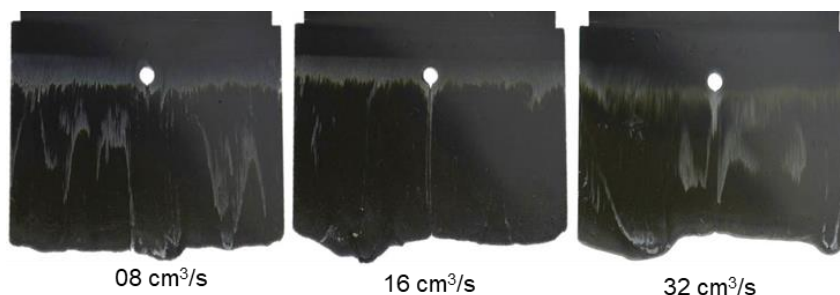


Figure 13. PF6506 (GF25+GB30); the mechanism for reuniting melt fronts behind the obstacle. Mold temperature of 175 °C is constant and Cavity volume is 70%

371  
372  
373

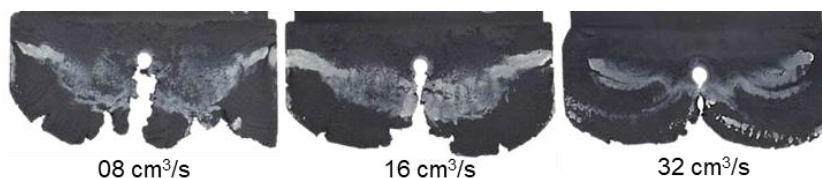


Figure 14. PF1110(GF35+GB45); the influence of injection speeds on the joining mechanism of the melt fronts behind an obstacle. Mold temperature of 175 °C is constant and Cavity volume is 50%

374  
375  
376

In contrast to PF6680 und PF6506, the injection speed has a great impact on the weld-line formation mechanism of PF1110 (Figure 14). At the lowest injection speed of 8 cm<sup>3</sup>/s, the melt fronts behind the obstacle flow and slip straightly in the flow direction. Therefore, the weld-line is not yet formed and there is a gap between the two melt fronts. As the

377  
378  
379  
380

injection speed increases in the gap between two melt front surfaces slightly decreases. At the highest injection speed of  $32 \text{ cm}^3/\text{s}$ , the melt fronts behind the obstacle start to reunite. These differences could be explained by analyzing the influence of the injection speed on the shear rate and slip phenomenon. The shear rate rises significantly with increasing injection speed. Therefore, the polymer molecules between the different layers are separated and move more easily in different direction, which together with the high slip velocity causes the melt fronts to move not only parallel to the flow direction, but also in other directions. Consequently, at the higher injection rate such as  $32 \text{ cm}^3/\text{s}$ , the melt fronts of PF1110 merge immediately behind the obstacle. The joined melt fronts slip strongly in the flow direction (Figure 15). Moreover, as the injection speed increases, the zone with the compacted polymer that is located near to the gate begins to appear. The surface of molded part in this zone is smooth. Specially, at the highest injection speed ( $32 \text{ cm}^3/\text{s}$ ), the joined melt fronts appear only on the compacted zone and slip to the end of molded part, as shown in Figure 16.

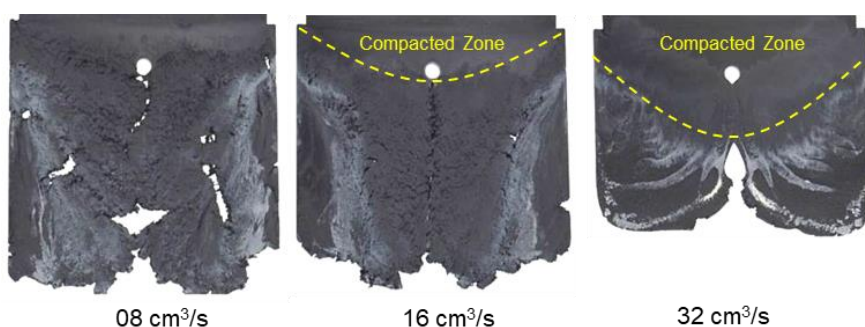


Figure 15. PF1110(GF35+GB45); the mechanism for reuniting melt fronts behind an obstacle. Mold temperature of  $175 \text{ }^\circ\text{C}$  is constant and Cavity volume is 70%

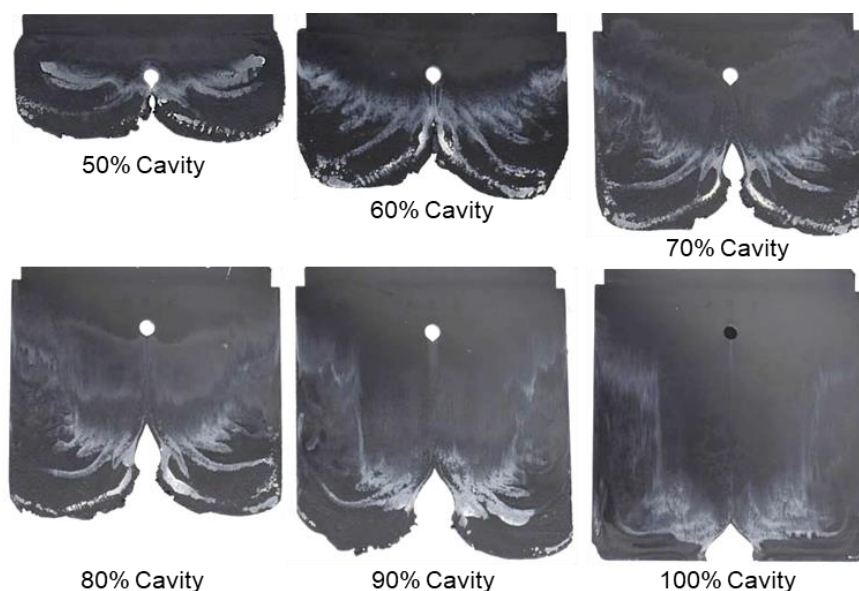


Figure 16. PF1110 (GF35+GB45); the mechanism for reuniting two melt fronts behind an obstacle. Mold temperature is  $175 \text{ }^\circ\text{C}$ , and injection speed is  $32 \text{ cm}^3/\text{s}$ .

According to the above analyzed experimental results on the mechanism of weld-line formation and development behind the obstacle of all investigated thermoset injection molding compounds, it could be concluded that the weld-line region is dependent strongly on the degree of wall slip that is directly affected by the filler content and processing conditions. For the thermoset injection molding materials with the filler content of less than 65% such as PF6680 (GF25+GB30) and PF6506 (GF30+GB30) the influence of

injection speed on the mechanism of weld-line is less than the thermoset injection molding materials with the filler content of more than 65% such as PF1110 (GF35+GB45). Especially, melt fronts of all investigated thermoset materials behind the obstacle at high injection velocity (for instance 32 cm<sup>3</sup>/s) merge immediately, which continue to slip in the flow direction. Increasing the filler content as well as the injection speed leads to a stronger slip of the joined melt fronts. Depending on the filler content reinforced for the thermoset material that is used to produce the industrial parts, as well as the expected weld line regions of the manufacturer, the lower or higher injection speed should be applied in the injection molding process.

### 3.3. Mold filling behavior in the spiral flow part

#### 3.3.1. Flow length



Figure 17. PF6680 (GF25+GB30) and PF1110 (GF35+GB45); the spiral molded part

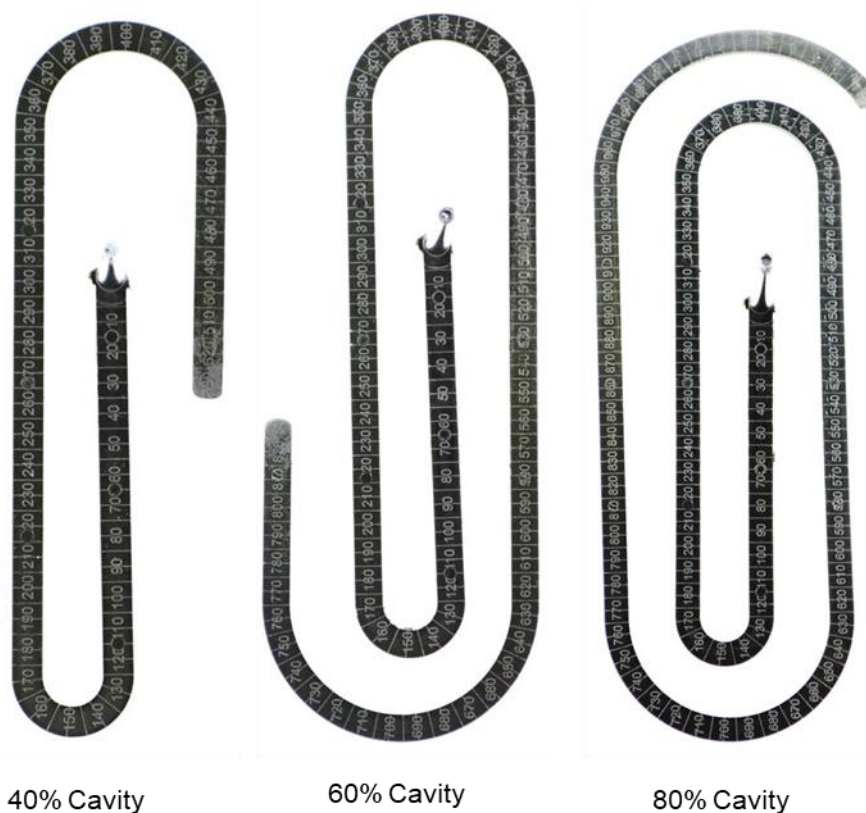


Figure 18. PF6680 (GF25+GB30); the flow length of spiral molded part with different cavity volume

For all investigated processing conditions, the spiral flow part with a flow length of 1385 mm is completely molded from both materials, PF6680 and PF1110 (Figure 17). The mold filling behavior like flow length of incomplete molded parts is shown in Figure 18

and Figure 19. Based on the surface of spiral molded parts, it could be found that the incomplete molded part of PF6680 is completely compacted (Figure 18) and there is not zone with uncompact thermoset melt. However, for PF1110, the uncompact zone with the roughness surface (Figure 19) is once again found near to the melt front, which was also appeared on the surface of incomplete plate molded parts, as previously shown from Figure 14 to Figure 16. Nevertheless, the length of the uncompact zone on the surface of the spiral part is much shorter than the length of the uncompact zone found on the surface of the plate part. This experimental result shows that there is not only the influence of processing conditions on the uncompact zone of highly filled thermoset injection molding compounds, but also the effect of the part geometry and the types of the gate. In this article, the film gate (Figure 3) was employed for the plate part while the direct sprue gate (Figure 4) was applied for the spiral flow part.

It could be seen from Figure 19 that the uncompact zone on the incomplete part molded from the lowest cavity volume (35% Cavity) emerge continuously at the end of the incomplete molded parts with higher cavity volumes (57% and 77% Cavity) and disappear on the complete molded spiral flow part (Figure 17), which is because of the plug flow behavior of PF1110 in the mold filling process. This experimental results demonstrates that the polymer region of PF1110 originated from the initial polymer portion which touched the mold surface will continuously flow to at the end of cavity. Therefore, the velocity of polymer melt on the interface between thermoset melt and mold wall surface is more than zero instead of zero that is found in the investigation of mold filling behavior of thermoplastics materials. Because of the wall slip in the filling process, a slip friction coefficient is generated on the interface between the thermoset melt and the wall surface, as well as between different thermoset layers across the thickness of the cavity. The slip frictional coefficient has a great effect on the pressure gradient and melt temperature distribution results that is presented in the following content.

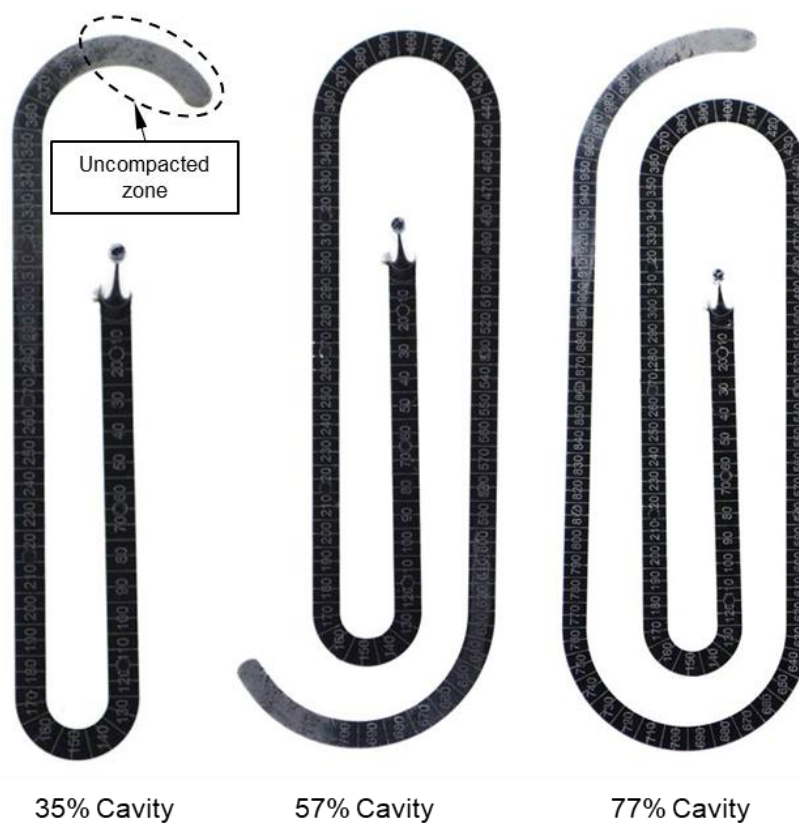


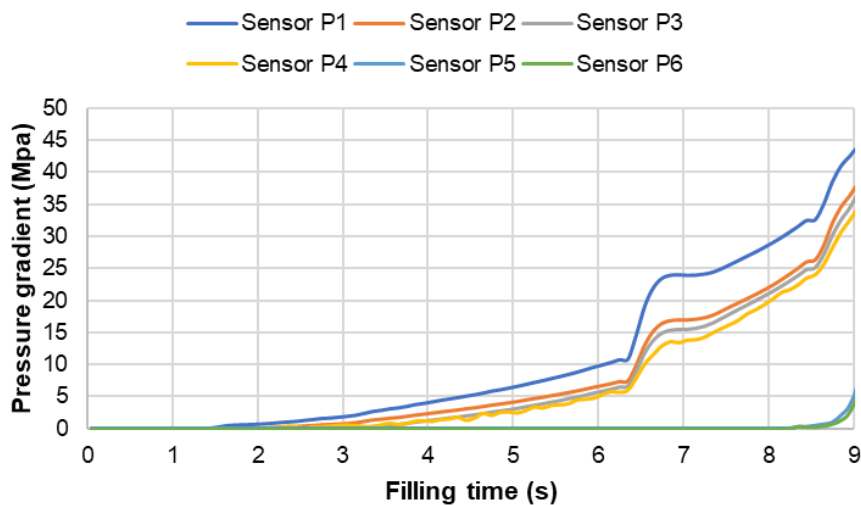
Figure 19. PF1110 (GF35+GB45); the flow length of spiral molded part with different cavity volume

425  
426  
427  
428  
429  
430  
431  
432  
433  
434  
435  
436  
437  
438  
439  
440  
441  
442  
443  
444  
445  
446  
447  
448  
449  
450

451  
452

3.3.2. Injection pressure gradient and melt temperature distribution

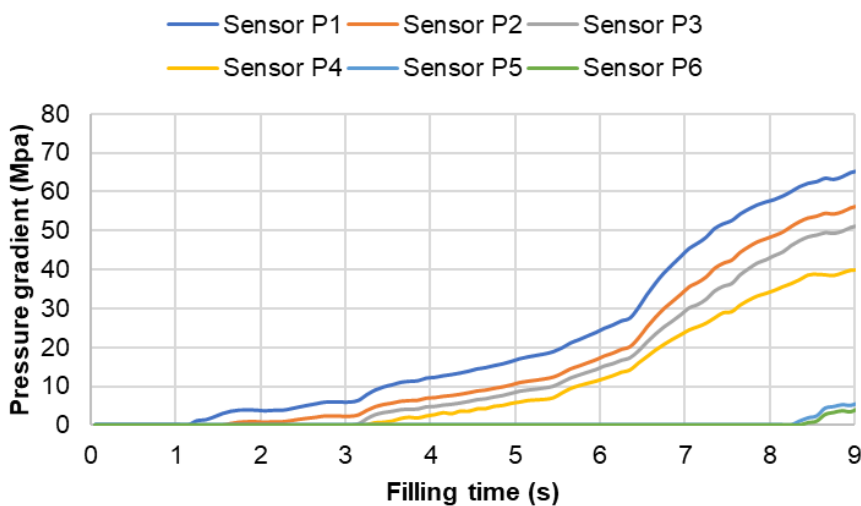
453



454

Figure 20. PF6680 (GF25+GB30); injection pressure gradient the filling phase

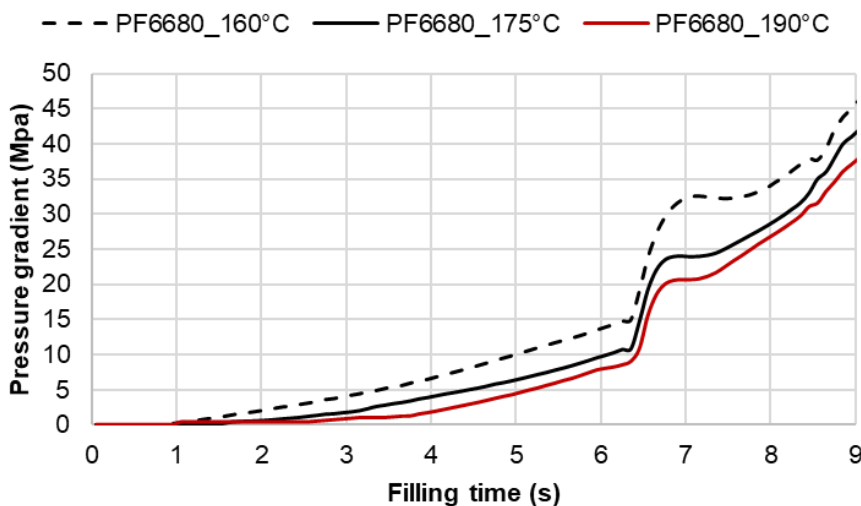
455



456

Figure 21. PF1110 (GF35+GB45); injection pressure gradient in the filling phase

457



458

Figure 22. PF6680 (GF25+GB35); injection pressure gradient in the filling phase under different mold temperatures

459

460

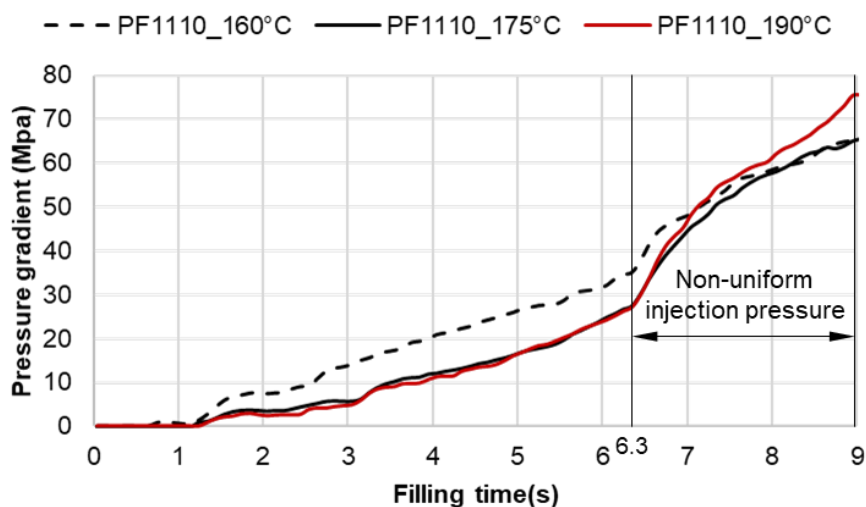


Figure 23. PF1110 (GF35+GB45); injection pressure gradient in the filling phase under different mold temperatures

461  
462  
463

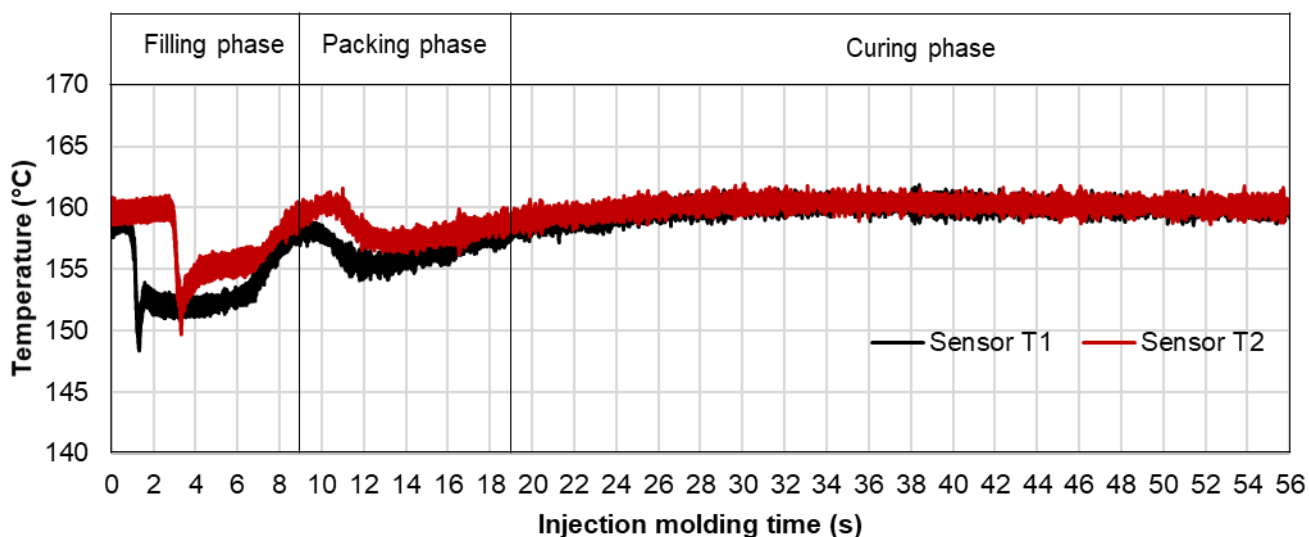


Figure 24. PF1110 (GF35+GB45); the temperature distribution in the injection molding process

464  
465

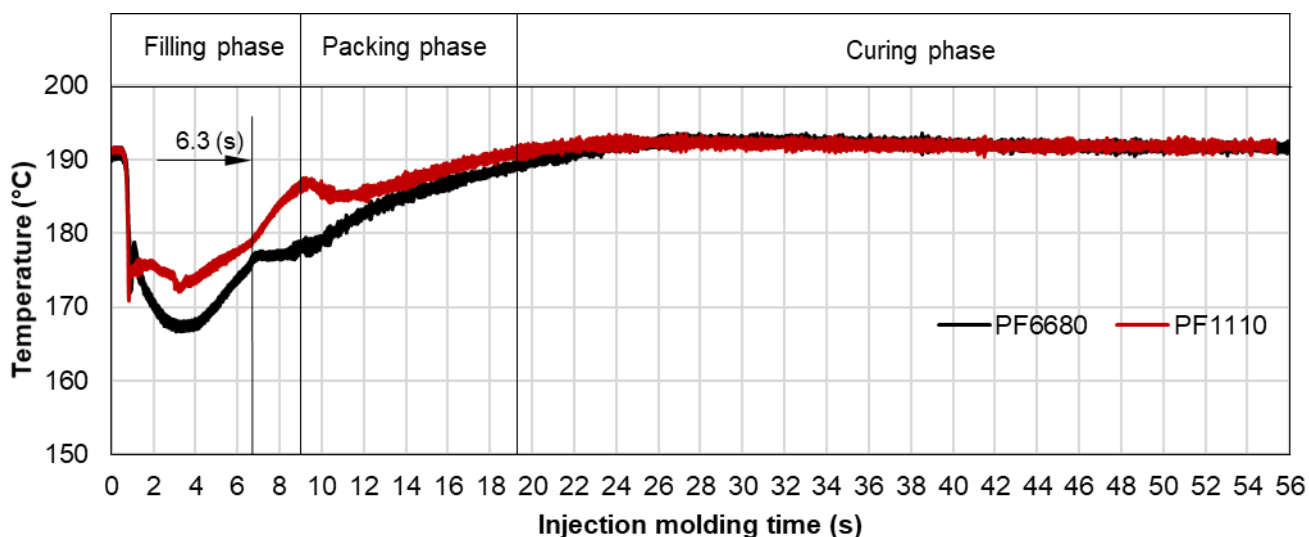


Figure 25. Comparison the melt temperature between PF6680 and PF1110

466  
467



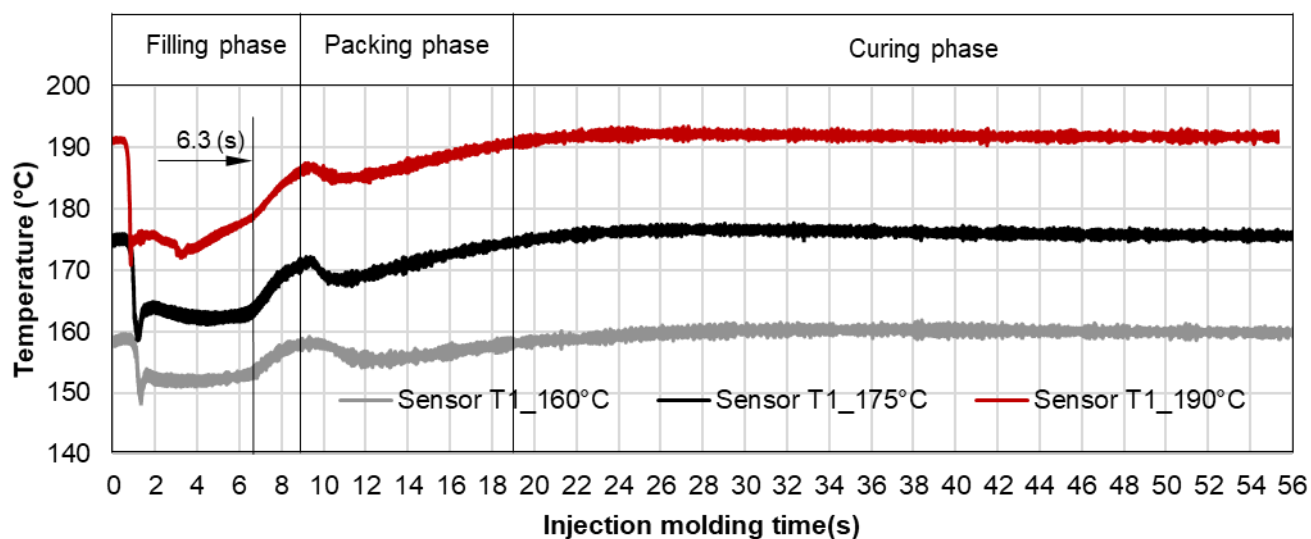


Figure 26. PF1110 (GF35+GB45); the temperature distribution in the injection molding process under different mold temperatures

Pressure and infrared sensors (Figure 4) were used in the experimental processes of the spiral flow part to study the influence of the flow disturbance that derives from the wall slip phenomenon on the variation of the pressure gradient and the temperature distribution of polymer melt in the injection molding process. The typical experimental result of pressure gradient is shown in Figure 20 and Figure 21. In the filling phase pressure drops per unit of length along the spiral flow path. The pressure drops from one location to another is the force that pushes the molten polymer to flow during the mold filling process. Polymer always moves from higher pressure to lower pressure like the water flowing from higher elevations to lower elevations. As a result, the maximum pressure is found in sensor P1 and the minimum pressure is found in sensor P6. However, difference in the injection pressure gradient in the mold filling behavior under the various investigated mold temperature between PF6680 and PF1110 is found and presented in Figure 22 and Figure 23.

The required injection pressure to push the molten thermoset flow during the filling phase is proportional to viscosity that is strongly dependent on the shear rate, temperature and the degree of cure. The injection pressure of PF6680 (Figure 22) decreases when increasing the mold temperature. This experimental result shows that in the mold filling process the viscosity of PF6680 is mainly dependent on the temperature and shear rate like thermoplastic materials. The degree of cure of PF6680 in the filling phase is very small or the curing process has not even started yet. Therefore, as the temperature in the filling phase increases, the viscosity of PF6680 decreases, leading to a decrease in the required injection pressure. However, the variation of injection pressure of PF1110 in Figure 23 does not follow the injection pressure variation rule of PF6680. At the mold temperature of 175 °C and 190 °C and during the 6.3 s of the filling phase the injection pressure is more or less the same, which is not found in the injection pressure gradient of PF6680. Furthermore, the injection pressure at the mold temperature of 190 °C from 6.3 s to the end of the filling phase (9 s) is higher than the injection pressure at the mold temperature of 175 °C. At the end of filling process, the maximum injection pressure is found at the highest mold temperature of 190°C, follow by at the mold temperature of 175 °C. The minimum injection pressure is found at the lowest mold temperature of 160°C.

The difference in the injection pressure variation between PF6680 and PF1110 could be explained based on the mold filling characterization. The mold filling behavior of PF1110 is complete plug flow. Therefore, the polymer region of PF1110 (the uncompacted zone) originated from the initial polymer portion which touched the mold surface

continues to flow to the end of cavity, as shown in Figure 19. As a result, the residence time of the initial polymer portion in the mold is higher than the fresh molten polymer portion that is just injected into the mold. During the flowing process, the temperature of the initial polymer portion increases quickly because the heat transfer from the hot mold to the molten polymer. Therefore, the melt temperature measured by the infrared temperature sensor 1 (T1) in the filling phase is always lower than the melt temperature measured by the infrared temperature sensor 2 (T2), as shown in Figure 24. In addition, it was found from Figure 25 that the melt temperature of PF1110 is higher than the melt temperature of PF6680 because the degree of wall slip phenomenon of PF1110 is stronger than PF6680.

At the beginning of the filling phase, the residence time and the temperature of the initial polymer portion is not enough for starting the curing process. Therefore, the viscosity of PF1110 at the beginning of filling phase dependences mainly on the temperature and shear rate like PF6680. After the 6.3 s, the residence time of the initial portion in the mold is now enough as long as the continuous heat transfer process from the hot mold to the molten polymer make the temperature of the initial polymer portion to reach the temperature for beginning the curing kinetic process. Therefore, the viscosity of PF1110 is now dependent not only on the temperature and shear rate but also mainly on the degree of cure. When the curing process begins, the viscosity of the thermoset melt rises significantly. The curing process in the filling phase is undesirable because it increases the viscosity fast and the initial polymer portion becomes slightly solid, which could lead to problems, such as flow hesitation, over-packing that results in flash. When mold temperature (Figure 26) is higher than 175 °C, the melt temperature of PF 1110 in the filling phase rises quickly, giving more opportunity for the start of the curing process in the filling phase. As a result, the viscosity of PF1110 begins rising slightly from 6.3 s to the rest of the injection molding time, which causes a non-uniform injection pressure at the end of filling phase, as found in Figure 23.

3.4. Validating simulation results and adapting simulation model

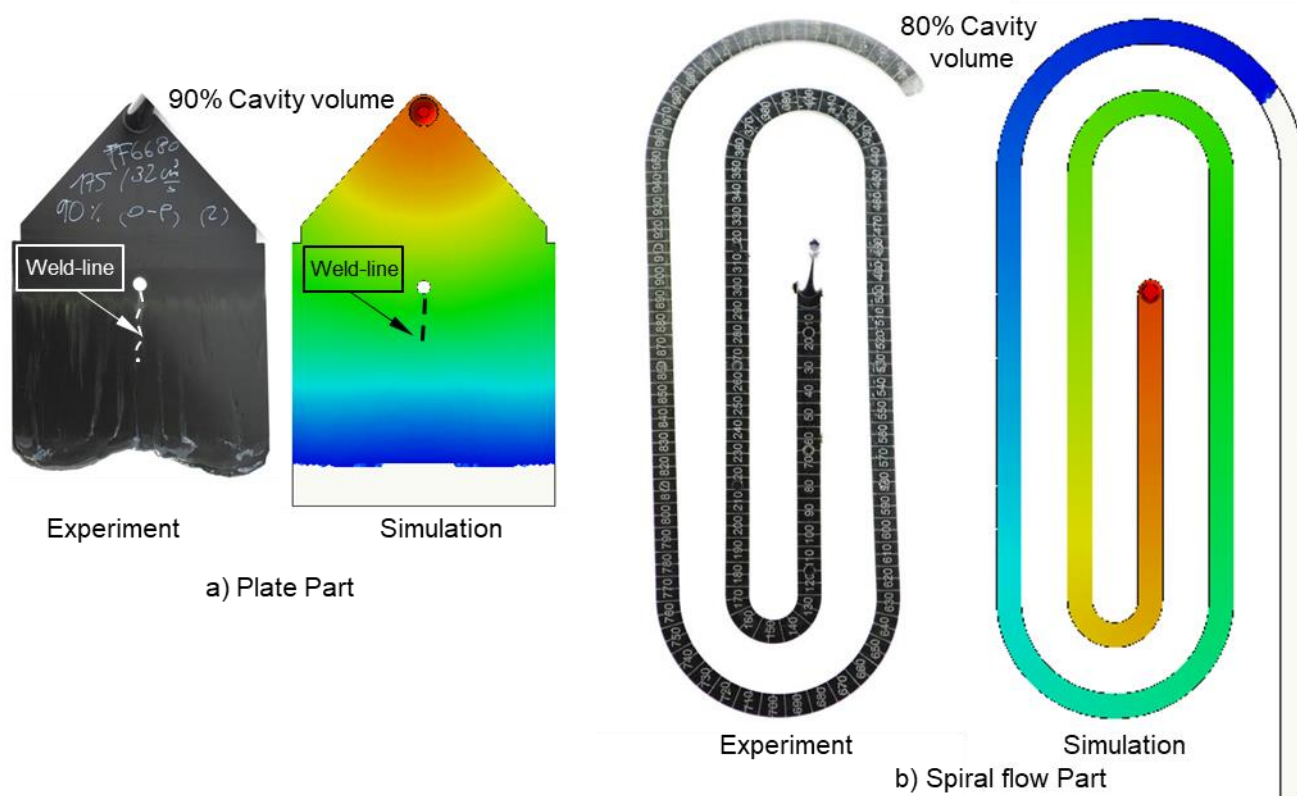


Figure 27. PF6680 (GF25+GB30); comparison between simulation and experimental results

505  
506  
507  
508  
509  
510  
511  
512  
513  
514  
515  
516  
517  
518  
519  
520  
521  
522  
523  
524  
525  
526  
527  
528  
529  
530  
531  
532  
533  
534

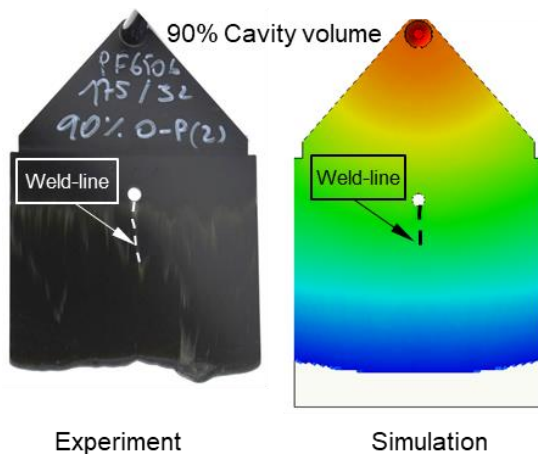


Figure 28. PF6506 (GF25+GB30); comparison between simulation and experimental results

535  
536



Complex industrial part from Baumgarten automotive technics GmbH,  
Carl-Benz Straße 46, 57299 Burbach, Germany

Figure 29. Complex industrial part; comparison between simulation and experimental results

537  
538

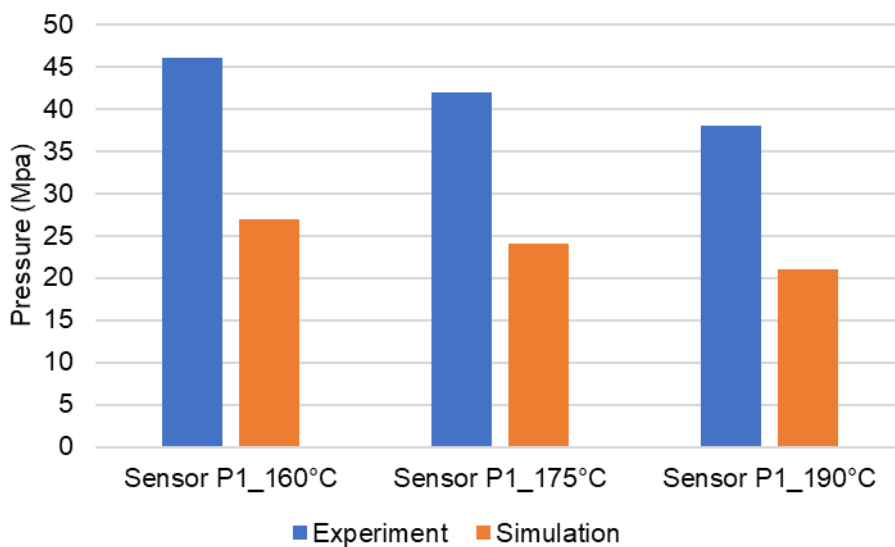


Figure 30. PF6680 (GF25+GB30); spiral flow part. Comparison between injection pressure simulation and experimental results at the end of filling process

539  
540  
541

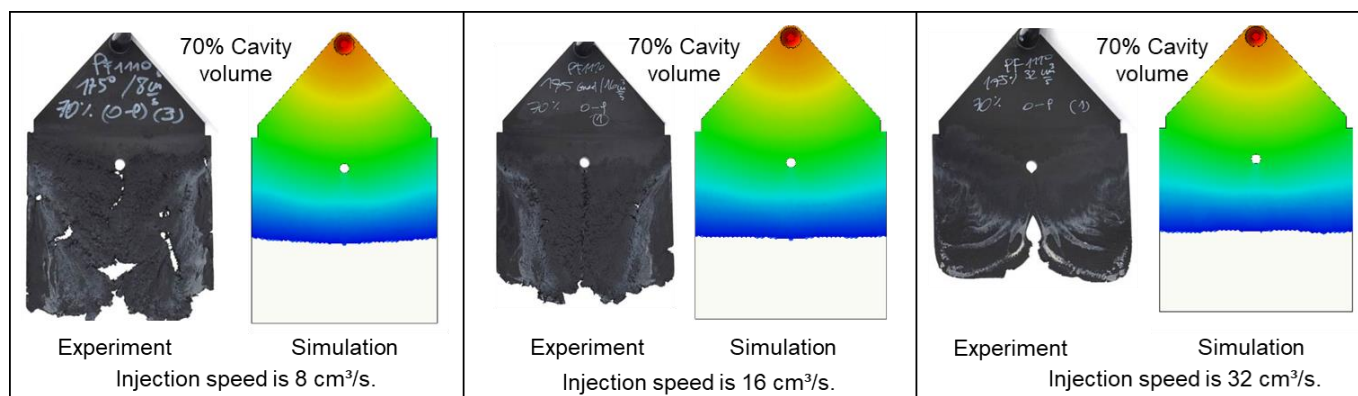


Figure 31. PF1110 (GF35+GB45); comparison between simulation and experimental results

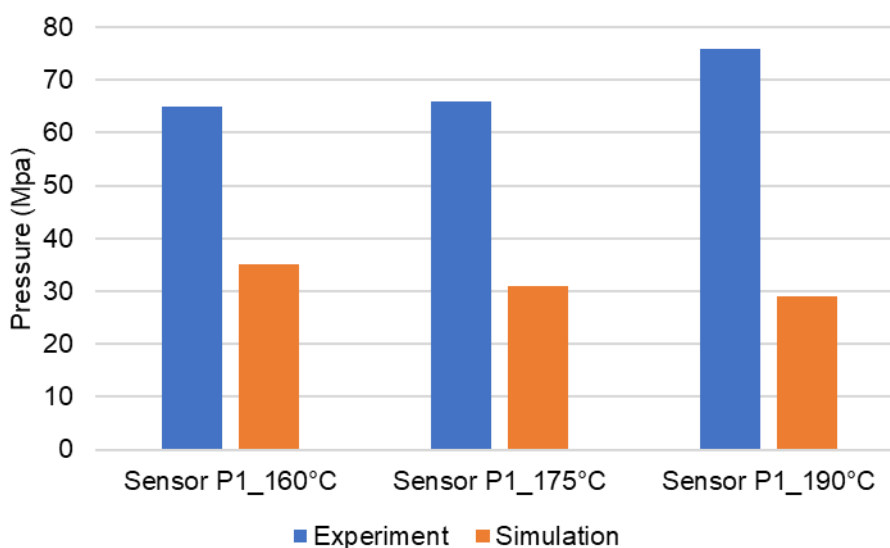


Figure 32. PF1110 (GF35+GB45); spiral flow part. Comparison between injection pressure simulation and experimental results at the end of filling process

The experimental results about weld-line formation and development of highly filled thermoset injection molding compounds behind the obstacle is presented and analyzed in the content 3.1 and content 3.2. It shown that the wall slips phenomenon, the filler content and process condition have great impact on the joining process of thermoset melt front surfaces. For the thermoset injection molding materials with the filler content of less than 65% such as PF6680 (GF25+GB30) and PF6506 (GF30+GB30), the melt fronts will be immediately reunited behind the obstacle. The weld-line is formed in the middle of the plate part. The position of experimental weld-line is more or less the same with the position of weld-line predicted from the simulation tool, as shown in Figure 27(a) and Figure 28. In addition, the weld-line positions of complex industrial part that was predicted by simulation tool is also found in a good agreement with the experimental results that was produced by experts in the field of thermoset injection molding from Baumgarten automotive technics GmbH (Figure 29). Furthermore, Figure 27(b) shows that the experimental flow length of the spiral flow part under different mold temperature is accurately predicted by simulation tool. The influence of mold temperatures on the viscosity that effects directly on the injection pressure is also successfully simulated by the simulation tool, which is also found in the experimental result (Figure 30). Especially, both simulation and experimental results show that with the high mold temperature, the viscosity of PF6680 in the filling phase decreases, leading to a decrease in the required injection pressure. These expected agreements show that the generated reactive viscosity data with the optimal developed viscosity model (Herschel-Bulkley-WLF- Castro- Macosko Model) and curing

kinetics model (Kamal model), which is previously presented in Figure 5 and Figure 6 is reasonable.

However, for the higher filled thermoset injection molding compounds (the filler content is more than 65%) such as PF1110 (GF35+GB45), the weld-line formation mechanism is different from the lower filled thermoset injection molding compounds like PF6680 (GF25+GB30) and PF6506 (GF30+GB30). The melt fronts are not completely reunited when the cavity volume does not reach 100%. There are always two zones on the surface of incomplete molded part, which are the compacted zone that is located near the gate (Figure 15) and the uncompacted zone that is located next to the compacted zone and it extends to the melt front. The positions of weld-line are dependent on the injection speeds which has great impact on the wall slip phenomenon. All these experimental results are not found in the simulated results (Figure 31). In addition, the uncompacted zone of incomplete molded parts that is affected by injection speeds and the mold temperatures has not yet been accurately simulated, as shown in Figure 31. Furthermore, the non-uniform injection pressure because of the curing behavior of PF1110 that is found in the experimental injection molding process of the spiral flow part and presented in Figure 23 could not predicted by the simulation tool. More specially it could be seen from Figure 32 that the experimental injection pressure at the end of filling process is proportional to the mold temperature, which is not found in the simulation results. The main reasons that could lead to these disagreements is the influence of wall slip phenomenon that generate the frictional coefficient between thermoset melt and the wall surface and a great effect on the mold filling characterization. However, the slip frictional coefficient could not be carefully considered in the writing simulation code of the currently commercial injection molding software. These disagreements are being studied and solved by authors.

#### 4. Conclusions

The mold filling behavior of highly filled thermoset injection molding compounds in the injection molding process such as weld-line formation, the reactive viscosity behavior, the injection pressure gradient and the temperature distribution is successfully investigated, which is strongly dependent on the filler content, the processing conditions and the wall slip phenomenon. The optimal injection speed (low or high injection speed) and mold temperature (low or high mold temperature) that is applied in the injection molding process must be based on an overall analysis of the manufacturer's expected weld-line areas, the filler content reinforced for the thermoset material that is used to produce the industrial parts and the geometry of the industrial parts, the type of injection gate as well as the gate location. For the thermoset injection molding compounds with the filler content of less than 65%, the effect of wall slip phenomenon and the processing conditions on the mechanism of weld-line formation is slight and could be neglected. The generated viscosity with the the optimal developed viscosity model, Herschel-Bulkley-WLF- Castro- Macosko Model, and curing kinetics model, Kamal model, was imported into in the commercial injection molding simulation tool to simulate successfully the form filling behavior of these materials. However, for the thermoset injection molding compounds with the filler content of more than 65%, the wall slip phenomenon, the mold temperature and injection speed have a great impact on the mold filling characterization such as formation and development of weld-lines, the compacted zone, the uncompacted zone and the pressure gradient and the curing behavior in the filling process, which has not yet been accurately simulated by the commercial simulation software. These problems are now leading to a real challenge for the fluid dynamic simulation tool.

**Author Contributions:** Conceptualization, T.N.T.; methodology, T.N.T, J.H and D.K.; investigation, T.N.T.; writing— original draft preparation, T.N.T.; writing—review and editing, A.S. and M.G.; visualization, T.N.T.; supervision, A.S and M.G.; funding acquisition, M.G. All authors have read and agreed to the published version of the manuscript.

**Funding:** The publication of this article was funded by the Chemnitz University of Technology and the Deutsche Forschungsgemeinschaft (DFG, German Research Foundation); grant number is GE 627/18-1; DFG project number is 437971453.

Institutional Review Board Statement: Not applicable.

**Data Availability Statement:** The data presented in this study are available on request from the corresponding author.

**Acknowledgments:** This research was funded by the Deutsche Forschungsgemeinschaft (DFG, German Research Foundation); grant number is GE 627/18-1; DFG project number is 437971453. We acknowledge financial support by the DFG. In addition, we would like to express sincere thanks to Mr. Hirz and Mr. Klaas from Baumgarten automotive technics GmbH, Carl-Benz Straße 46, 57299 Burbach, Germany. They gave us the opportunity and cooperated with us to study the mold filling behavior of a complex industrial part.

**Conflicts of Interest:** The authors declare no conflict of interest.

## References

1. Wieland, C.; Topic, N.; Hirz, J. More precision for sensitive fast curing compounds. *Kunststoffe*. 2018, 20-23.
2. Osswald, T. A.; Menges, G. *Materials Science of Polymers for Engineering*; Carl Hanser: Munich, Germany, 2003.
3. Haagh, G. A. A. V.; Peters, G. W. M.; Meijer, H. E. H. Reaction injection molding: Analyzing the filling stage of a complex product with highly viscous thermoset. *Polym. Eng. Sci.* 1996, 36, 2579-2588.
4. Pilato, L. *Phenolic Resins: A Century of Progress*, Springer-Verlag, Berlin Heidelberg, 2010.
5. Yao, L.; Gehde, M. Evaluation of heat transfer coefficient between polymer and cavity wall for improving cooling and crystallinity results in injection moulding simulation. *Applied Thermal Engineering*. 2015, 80, 238-246.
6. W, Michaeli. *Plastics processing: An Introduction*, Carl Hanser: Munich, Germany, 1995.
7. R, Han.; L, Shi.; M, Gupta. Three-dimensional simulation of microchip encapsulation process. *Polymer Engineering and Science*. 2000, 40, 776-785.
8. Wu, C.Y.; Ku, C.C.; Pai, H.Y. Injection molding optimization with weld line design constraint using distributed multi-population genetic algorithm. *The International Journal of Advanced Manufacturing Technology*. 2011, 52, 131-141.
9. Xie, L.; Ziegmann, G. Mechanical properties of the weld line defect in micro injection molding for various nano filled polypropylene composites. *Journal of Alloys Compounds*. 2011, 509, 226-233.
10. Ozcelik, B. Optimization of injection parameters for mechanical properties of specimens with weld line of polypropylene using Taguchi method. *International Communications Heat Mass Transfer*. 2011, 38, 1067-1072.
11. Kitayama, S.; Tamada, K.; Takano, M.; Aiba, S. Numerical and experimental investigation on process parameters optimization in plastic injection molding for weldlines reduction and clamping force minimization. *The International Journal of Advanced Manufacturing Technology*. 2018, 97, 2087-2098.
12. Nguyen-Chung, T. Strömungsanalyse der Bindenahtformation beim Spritzgießen von thermoplastischen Kunststoffen, PhD Thesis, Universitätsverlag der Technischen Universität Chemnitz, TU Chemnitz, Chemnitz. 2002.
13. Malguarnera, S.; Manisali, A. The effects of processing parameters on the tensile properties of weld lines in injection molded thermoplastics. *Polymer Engineering and Science*. 1981, 21, 586-593.
14. Malguarnera, SC. Weld lines in polymer processing. *Polymer-Plastics Technology and Engineering*. 1982, 18:1-45
15. Onken, J.; Hopmann, C. Prediction of weld line strength in injection-moulded parts made of unreinforced amorphous thermoplastics. *International Polymer Science and Technology*. 2016, 43: T1.
16. Tomari, K.; Tonogai, S.; Harada, T.; Hamada, H.; Lee, K.; Morii, T.; Maekawa, Z. The V-notch at weld lines in polystyrene injection moldings. *Polymer Engineering and Science*. 1990, 30, 931-936
17. Zhao, Y.; Mattner, T.; Drummer, D. Investigation of the effects of pre-cross-linked thermoset molding compounds on weld line strength in injection molding. *The International Journal of Advanced Manufacturing Technology*. 2019, 105, 1723-1733.
18. Tran, N. T.; Gehde, M. Visualization of wall slip during thermoset phenolic resin injection molding. *The International Journal of Advanced Manufacturing Technology*. 2018, 95, 4023-4029.
19. Tran, N. T.; Gehde, M. Creating material data for thermoset injection molding simulation process. *Polymer Testing*. 2019, 73, 284-292.
20. Tran, N. T. Creating material properties for thermoset injection molding simulation process. PhD Thesis, Universitätsverlag der Technischen Universität Chemnitz. TU Chemnitz, Chemnitz. 2020.
21. Tran, N. T.; Gehde, M. Bewertung der aktuellen eingesetzten reaktiven Viskositätsmodelle zur rheologischen Simulation im Spritzgießprozess. in *Technomer Fachtagung über Verarbeitung und Anwendung von Polymeren*, Chemnitz, 2021.

- 
22. Tran, N. T.; Gehde, M. Modelling of rheological and thermal properties for thermoset injection molding simulation process (the full article has been accepted for publication), *AIP Publisher Conference Proceedings* (37th International Conference of the Polymer Processing Society, Fukuoka, Japan), 2022. 672  
673  
674
  23. Tran, N.T.; Seefried, A.; Gehde, M. Investigation of the Influence of Fiber Content, Processing Conditions and Surface Roughness on the Polymer Filling Behavior in Thermoset Injection Molding. *Polymers*. 2023, 15 (5), 1244. 675  
676
  24. Koszkuł, J.; Nabialek, J. Viscosity models in simulation of the filling stage of the injection molding process. *Journal of Materials Processing Technology*, 2004, 157, 183-187. 677  
678
  25. Englich, S. Strukturbildung bei der Verarbeitung von glasfasergefüllten Phenolformaldehydharzformmassen. PhD Thesis, Universitätsverlag der Technischen Universität Chemnitz, TU Chemnitz, Chemnitz. 2015. 679  
680
  26. Scheffler, T. Werkstoffeinflüsse auf den Spritzgussprozess von hochgefüllten Phenol-Formaldehydharz-Formmassen, PhD Thesis, Chemnitz: Technische Universität Chemnitz, 2018. 681  
682
  27. Marquardt, D.W. An algorithm for least – squares estimation of nonlinear parameters, *J. Soc. Indust. Appl. Math.* 1963, 11, 431 – 441. 683  
684
  28. P.K. Kennedy,P.K.; Zheng, R. *Flow analysis of injection molds*, Carl Hanser: Munich, Germany, 2013. 685